

Review

Covalent Organic Framework-Based Electrolytes for Lithium Solid-State Batteries—Recent Progress

Tomasz Polczyk  and Atsushi Nagai *Ensemble³ Centre of Excellence, Next-Generation Energy Systems Group, Wólczyńska 133, 01-919 Warsaw, Poland

* Correspondence: atsushi.nagai@ensemble3.eu

Abstract: Covalent organic frameworks (COFs) have emerged as a promising platform of materials for solid-state battery electrolytes due to their porous and robust structures, and their special spaces such as 1D and 3D, as well as their ability to be modified with functional groups. This review focuses on the use of COF materials in solid-state batteries and explores the various types of bonds between building blocks and the impact on key properties such as conductivity, transfer number, and electrochemical stability. The aim is to provide an overview of the current state of COF-based electrolytes for solid-state batteries and to highlight the prospects for future development in this field. The use of COF materials in solid-state batteries has the potential to overcome limitations such as low theoretical energy density, limited temperature stability, and the risk of fire and explosion associated with traditional liquid electrolyte batteries. By providing a more in-depth understanding of the potential applications of COF-based electrolytes in solid-state batteries, this review seeks to pave the way for further advancements and innovations in this field.

Keywords: COF; electrolytes; solid-state batteries; solid-state electrolytes; 2D organic materials



Citation: Polczyk, T.; Nagai, A. Covalent Organic Framework-Based Electrolytes for Lithium Solid-State Batteries—Recent Progress. *Batteries* **2023**, *9*, 469. <https://doi.org/10.3390/batteries9090469>

Academic Editors: Maria Christy and Zahoor Ul Hussain Awan

Received: 26 July 2023

Revised: 4 September 2023

Accepted: 6 September 2023

Published: 18 September 2023



Copyright: © 2023 by the authors. Licensee MDPI, Basel, Switzerland. This article is an open access article distributed under the terms and conditions of the Creative Commons Attribution (CC BY) license (<https://creativecommons.org/licenses/by/4.0/>).

1. Introduction

The challenge of energy storage and conversion is a critical issue that plays a pivotal role in addressing the demands of the modern world. As renewable energy sources continue to gain prominence, the need for efficient energy storage systems becomes increasingly important. While pumped storage hydropower plants currently provide a dominant part of the global energy storage capacity, there are limitations and geographical constraints associated with these types of installations. To overcome these limitations, there is a pressing need to develop advanced energy storage technologies. Among the many interesting energy storage technologies like gravitational energy (pumped hydro and others like energy vault facilities), compressed gas storage, flywheels, and energy-to-hydrogen conversion, electrochemical methods have well-established positions and seem to have had the biggest impact on everyday human life [1]. These methods offer a versatile and scalable solution for energy storage, with applications in small devices, vehicles, and large installations. Among the electrochemical methods worthy of mention are supercapacitors [2] and electricity-to-chemicals (e.g., H₂ [3]) methods, but the dominant technology in this field is lithium-ion batteries, which were commercialized in 1991 [4]. From 1991, lithium-ion battery technology has changed, with novel cathode materials being applied (like NCA, NCM, LFP, etc.) and different anode materials being tested (graphite, hard carbon, silicon, indium, lithium titanate, etc. [5]). Apart from finding new electrode materials, different methods, like covering cathode particles with TiO₂ [6] or the preparation of nanosized materials [7], have been tested for improving the properties of well-known materials. However, the lithium-ion battery technology has reached its theoretical limits and faces fast charging and safety concerns like the flammability of liquid electrolyte, Li dendrite growth on anodes, fast charging issues, and a narrow temperature operating

window. Among other proposed solutions like metal-ion batteries (Na, K, Al, Mg, Zn, and etc.), different cell architectures like Li-S, Li-Se, and Li-O₂ solid-state batteries (SSBs) have emerged as the most promising alternatives [8–17]. By replacing liquids with solid electrolytes, SSBs have the potential to increase energy density (for Li 3860 mAh/g vs. graphite 372 mAh/g). Solid-state electrolytes (SSEs) are non-flammable and less prone to leakage or thermal runaway, which reduces the risk of battery fires and explosions. This makes solid-state batteries safer to use, especially in applications where safety is critical, such as electric vehicles. SSEs typically exhibit better stability and conductivity over a wide range of temperatures compared to liquid electrolytes. Therefore, solid-state batteries are suitable for use under harsh temperature conditions. Furthermore, SSEs have the potential to enable the use of high-voltage cathode materials, which can further increase the energy density and the performance of batteries [11].

The development of solid-state batteries (SSBs) necessitates utilization of a solid electrolyte that possesses several key characteristics. One crucial attribute is high ionic conductivity, as it enables efficient movement of ions within the battery, facilitating the transfer of charge and enhancing the overall performance of the device. Additionally, a high transference number is desirable, as it ensures that the majority of the current is carried by the ions through an electrolyte, thereby minimizing side reactions and improving the battery's efficiency. Achieving excellent electrode–electrolyte contact is another important aspect in SSBs. A robust and intimate interface between the electrolyte and electrodes promotes efficient charge transfer and enhances the overall electrochemical performance of a battery. Furthermore, a solid electrolyte must exhibit thermal and chemical stability when in contact with the electrodes, ensuring long-term durability and preventing degradation or irreversible reactions that could lead to capacity loss. To meet environmental and safety requirements, non-toxicity and low-cost materials are also important for SSEs. Currently, there is no material that meets all of these requirements simultaneously. Sulfide-based compounds, such as Li₁₀GeP₂S₁₂ (LGPS), exhibit high conductivity (10^{−2} S·cm^{−1}), but they have low oxidation stability [18]. Oxide-based systems, like perovskite Li_{3x}La_{2/3−x}TiO₃ (LLTO), have good bulk conductivity (10^{−3} S·cm^{−1}), but they are unstable against metallic lithium and face grain boundary transportation issues [19–21]. Garnet systems like Li₇La₃Zr₂O₁₂ (LLZO) are stable against Li and have good conductivity, but they suffer from inter-grain lithium dendrite growth during charging [22]. Polymer-based materials, including organic solids, are considered to be the closest candidates for new SSB electrolytes, but they generally have low transference numbers, poor conductivity, and moderate thermal stability [23].

Interesting types of organic-based materials are covalent organic frameworks (COFs). COFs are similar to metal–organic frameworks (MOFs) that are more recognized in the literature. The application of MOFs in electrolytes is not the main topic of this review and is well described elsewhere, for example [24–26]. COFs exhibit high thermal and chemical stability, and therefore they are suitable for ensuring the safety and longevity of batteries. The porous nature of COFs provides the pathways for ions to move through an electrolyte, facilitating the flow of charge and enhancing the overall performance of a battery [27–29]. Another advantage of COFs is their tunable functionality and the ability to introduce different functional groups into their framework, which allows optimization of their performance not only as solid-state electrolytes in batteries but also for supercapacitors and fuel cells [30–32]. In the subsequent sections of this publication, we focus on detailing COF-based materials by considering the nature of the bonding of their constituent building blocks. Our attention is particularly directed toward properties significant for electrolyte considerations, notably conductivity, transference number, electrochemical stability, the factors influencing these parameters, and methods of improving properties.

2. COF Solid-State Electrolytes

As mentioned earlier, the electrolyte plays a crucial role in solid-state batteries (SSBs). Extensive research has been conducted by scientists to identify optimal building blocks,

preparation routes, and functional groups for covalent organic frameworks (COFs) as potential electrolyte materials [33]. Among other methods, COFs can be categorized based on the types of chemical bonds present within their structures. These include B-O bonds, such as boronate ester, boroxine, borosilicate, and spiroborate; C-N bonds, including imine, imide, hydrazone, amide, β -ketoenamine, azine, phenazine, squaraine, viologen, triazine, and melamine; C-C bonds; borazine (B-N) bonds; and azodioxide (N-N) bonds [33]. Each type of chemical bonds imparts unique properties to a COF, influencing its overall performance as an electrolyte material.

While there is a wealth of information in the literature on the application of COF-based materials in electrode materials for electrochemical cells [34–37], there is a relative lack of comprehensive summaries that specifically address the use of COFs as electrolytes for lithium metal solid-state batteries. This paper endeavors to bridge this gap by centering its attention on COF electrolytes and their crucial properties, including but not limited to ionic conductivity, transference number, and electrochemical stability.

2.1. C-N Linkage

Among the various types of COFs, those containing nitrogen bonds have garnered significant attention due to their distinct properties and potential benefits in electrolyte applications. Nitrogen atoms can participate in chemical bonding, forming diverse linkages such as imine, hydrazone, amide, and triazine. The inclusion of nitrogen atoms within the COF structure introduces several advantages. A key advantage of nitrogen-containing COFs is their facilitation of ion transport. The presence of nitrogen atoms enhances the coordination and migration of ions within the material, resulting in improved ionic conductivity. This property is crucial for efficient ion transport in solid-state electrolytes, enabling faster charge and discharge rates in batteries. Moreover, nitrogen-based COFs exhibit exceptional stability and chemical inertness, which are vital for ensuring the reliable and safe operation of batteries. The incorporation of nitrogen atoms enhances the structural integrity and thermal stability of COFs, enabling them to withstand harsh operating conditions. In the next subsections, actual examples from the literature that have chosen C-N bond formation are presented.

2.1.1. Imine Bond

The imine type of bond has received significant attention in the literature. An imine linkage is known for its stability and ease of formation between primary amine and C_3 -symmetric trialdehyde benzene and its derivatives. Nitrogen, with its available electron pair, serves as a donor and is particularly useful for stabilizing cations such as Li^+ , Na^+ , and others. Imine groups act as a chromophore group and products typically range in color from yellow to red. Additionally, the presence of imine groups imparts chromophoric properties to the COFs, resulting in a range of colors from yellow to red because of the extension of conjugation along the double bonds of imine bonds ($C=N$) of their products. These examples highlight the versatility and potential of imine-based COFs in various fields, including electrolytes. In the examples presented in this subsection, we aim to demonstrate the potential applications of imine bond-type COFs as electrolytes.

The simplest building blocks used in COFs are 1,3,5-triformylbenzene (TB) and 1,4-diaminobenzene (TP). Xu et al. [38] investigated a COF material derived from TB and TP. In their study, the authors addressed the issue of lithium dendrite growth during lithium plating on the anode when using a typical liquid electrolyte. In batteries cycled with a standard liquid electrolyte, a protective solid electrolyte interphase (SEI) is formed. However, under high-current charging, the SEI can decompose, leading to the growth of dendritic lithium crystals through the electrolyte. To address this issue, the authors proposed an artificial “SEI” in their study [38]. They coated a copper current collector with TB-TP soaked in LiTFSI using spin coating and performed lithium plating between the copper and COF. Subsequently, the authors conducted stripping/plating cycling experiments. The results showed no formation of lithium dendrites and a dense and uniform layer of lithium.

The authors reported a transference number of 0.85, as compared to 0.35 for 1 M LiTFSI in DOL/DME, indicating that this material could effectively function as an electrolyte. However, ionic conductivity was not measured in this study.

Hu et al. [39] proposed an imine-type COF linked with an imidazole-containing diamine crosslinked with 1,3,5-triformylbenzene, as shown in Figure 1. The imidazole moiety was modified with methyl, proton, or fluorinated groups. The materials were synthesized using ethanol, mesitylene, and acetic acid heated to 120 °C for 3 days, which resulted in yields ranging from 63% to 85%.

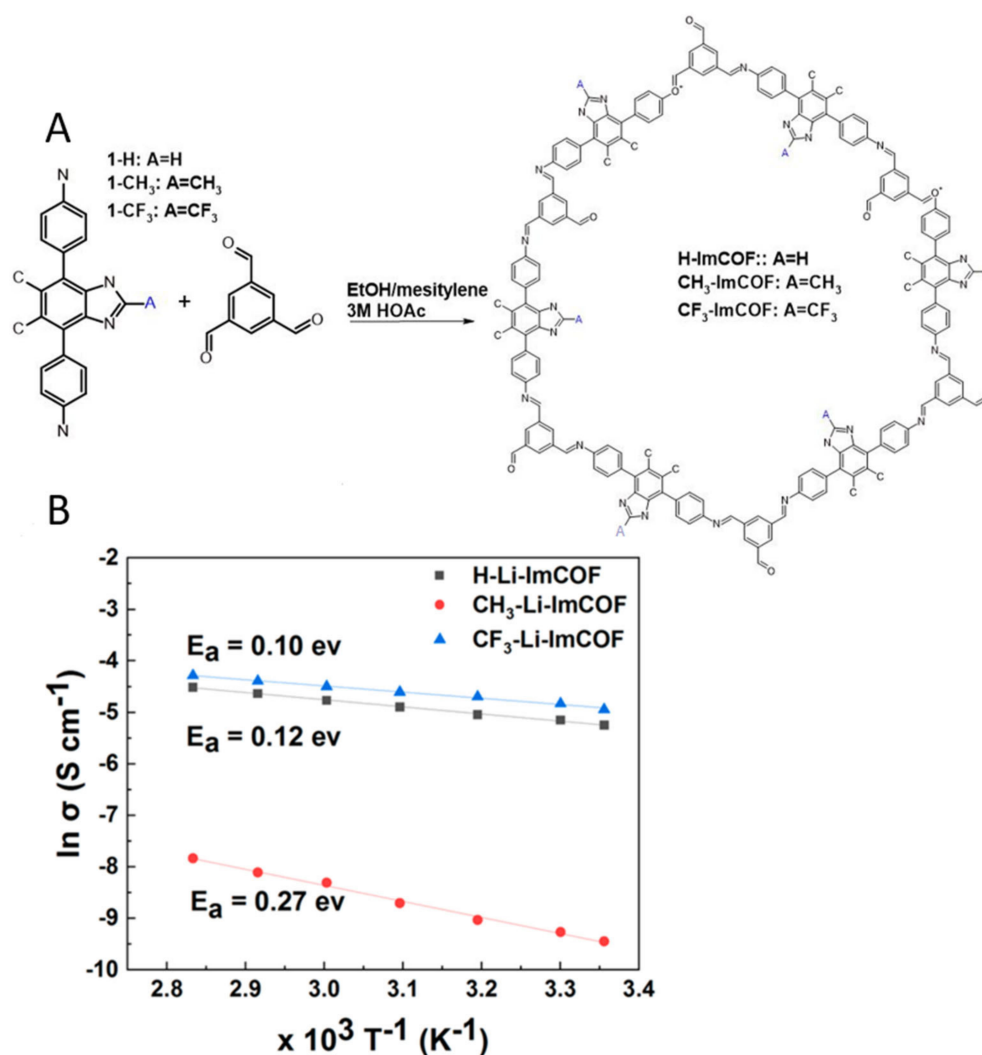


Figure 1. (A) Scheme of X-ImCOF preparation; (B) conductivity measurement of lithiated samples. Adaptation with permission from [39]. Copyright 2019 American Chemical Society.

To incorporate lithium ions, the presented COF materials were lithiated using *n*-BuLi in hexane in an ice bath. A thermogravimetric analysis (TGA) indicated that the samples remained stable up to 450 °C before lithiation and up to 400 °C afterwards. The unsubstituted imidazole COF exhibited a lithium transference number $t_{Li^+} = 0.88$. Substituting with CH₃ and CF₃ groups increased the transference numbers to 0.93 and 0.81, respectively. The symmetrical Li electrode cells demonstrated excellent stability. Linear sweep voltammetry measurements revealed a wide electrochemical window ranging from 0 to 4.5 V vs. Li/Li⁺. The samples exhibited modest conductivity of approximately 10⁻⁷ S·cm⁻¹; however, a significant increase was observed after mixing with 20% wt polycarbonate (PC). PC as a polar solvent facilitated the dissociation of weakly bound Li ions from the insoluble COF skeleton, thereby enhancing Li mobility. The treated COFs

exhibited impressive room temperature ionic conductivities of $7.2 \times 10^{-3} \text{ S}\cdot\text{cm}^{-1}$ and $5.3 \times 10^{-3} \text{ S}\cdot\text{cm}^{-1}$ for CF_3 and unsubstituted COF.

Niu et al. [40] proposed synthesizing triazine containing block (2,4,6-tris(4-aminophenyl)-1,3,5-triazine, (TAPT)) and fluorinated dialdehyde (2,3,5,6-tetrafluoroterephthaldehyde (TFTA)) in solvothermal conditions via Schiff-base reaction. The obtained material (I-COF) showed significant porosity of $2013 \text{ cm}^2 \text{ g}^{-1}$ with an average pore size of 32 \AA , and it had thermal stability up to around $325 \text{ }^\circ\text{C}$. The authors proposed an interesting idea of modifying imine bonds by conversion via the Povarov method into quinoyl bonds that involved an additional styrene group (Q-COF). Both I-COF and Q-COF were high crystallinity materials, and the Q-COF modification decreased porosity to $1242 \text{ cm}^2 \text{ g}^{-1}$ and pore size to 26 \AA , while thermal stability was increased, up to $400 \text{ }^\circ\text{C}$. After loading pores with LiTFSI solution, the THF ionic conductivity reached $5.3 \times 10^{-3} \text{ S}\cdot\text{cm}^{-1}$ at $30 \text{ }^\circ\text{C}$, and the material showed a wide electrochemical window of 5.6 V vs. $\text{Li} | \text{Li}^+$. These works show the potential of COF post-synthesis functionalization.

One-dimensional channels are one of the main advantages of 2D COF types of materials, such as, for example, the imine bond of 1,3,5-tris(4-aminophenyl)benzene (TAPB) with 2,5-dimethoxyterephthalaldehyde (DMTP) (Figure 2) [14,41]. In this paper [14], the authors pointed out the problems of dissolution and migration of Li_2S_6 through typical electrolytes in Li-S batteries. A Cergard separator with TAPB-DMTP-COF coating helped with proper separation of the molecules and prevented cell capacity degradation due to the charging/discharging process. Although the authors in the paper showed an interesting application of a COF using it as a coating material for separators, the conductivity was not reported. The authors in the next paper [41] presented interesting host properties of TAPB-DMTP-COF for a polymeric ionic liquid/ionic liquid (PIL/IL) electrolyte. The authors reported high porosity of TAPB-DMTP-COF, reaching $2096 \text{ cm}^2 \text{ g}^{-1}$, which allowed the introduction of the electrolyte into the cavities of the COF. The optimization of the PIL/IL/COF ratio of 10/20/1 had the highest conductivity, reaching $2.8 \times 10^{-4} \text{ S}\cdot\text{cm}^{-1}$ at $30 \text{ }^\circ\text{C}$. In the symmetrical cell with lithium metal electrodes, the electrolyte presented stable working with 0.1 mA cm^{-2} over 250 cycles at elevated temperatures ($60 \text{ }^\circ\text{C}$). The setup with the LiFePO_4 cathode also presented good performance which provided proof of the immense possibilities of using this electrolyte in SSB.

Another COF material was synthesized from thiophene containing aldehyde (5-[3,5-bis(5-formylthiophen-2-yl)phenyl]thiophene-2-carbaldehyde) (3TB) and three types of C_3 -symmetric primary amines: 1,3,5-tris(4-aminophenyl)benzene (TAPB); 1,3,5-tris(4-aminophenyl)amine (TAPA); and 2,4,6-tris(4-aminophenyl)-1,3,5-triazine (TAPT) [42]. The products were synthesized at $120 \text{ }^\circ\text{C}$ for 3 days in the mixed solvents of *o*-DCB and *n*-BuOH in the presence of acetic acid as a catalyst. All compositions showed crystalline structures with AA stacking structure with stability up to $400 \text{ }^\circ\text{C}$. 3TB-TAPB denoted as COF-NUST-7 presented high porosity reaching $1214 \text{ m}^2\cdot\text{g}^{-1}$, and the other compositions reached only 92 and $95 \text{ m}^2\cdot\text{g}^{-1}$. After introducing LiTFSI solution in ionic liquid (1-butyl-1-methylpyrrolidinium bis-(trifluoromethanesulfonyl)imide), the COF channels' electrochemical properties were investigated. Ionic conductivity was measured in the $40\text{--}120 \text{ }^\circ\text{C}$ range at 7 MHz to 0.1 Hz frequency range. Their conductivities presented $8.7 \times 10^{-5} \text{ S}\cdot\text{cm}^{-1}$, $1.4 \times 10^{-4} \text{ S}\cdot\text{cm}^{-1}$, and $2.2 \times 10^{-4} \text{ S}\cdot\text{cm}^{-1}$ for COF-NUST-7, COF-NUST-8 (3TB-TAPT), and COF-NUST-9 (3TB-TAPA), at $40 \text{ }^\circ\text{C}$, respectively. They presented the stability of ionic conductivity over time at $120 \text{ }^\circ\text{C}$ and high electrochemical stability up to 3.4 V vs. $\text{Li} | \text{Li}^+$. The authors also demonstrated full battery performance with LiFePO_4 cathode at $100 \text{ }^\circ\text{C}$ compared to PEO polymer electrolyte, leading to superior stability.

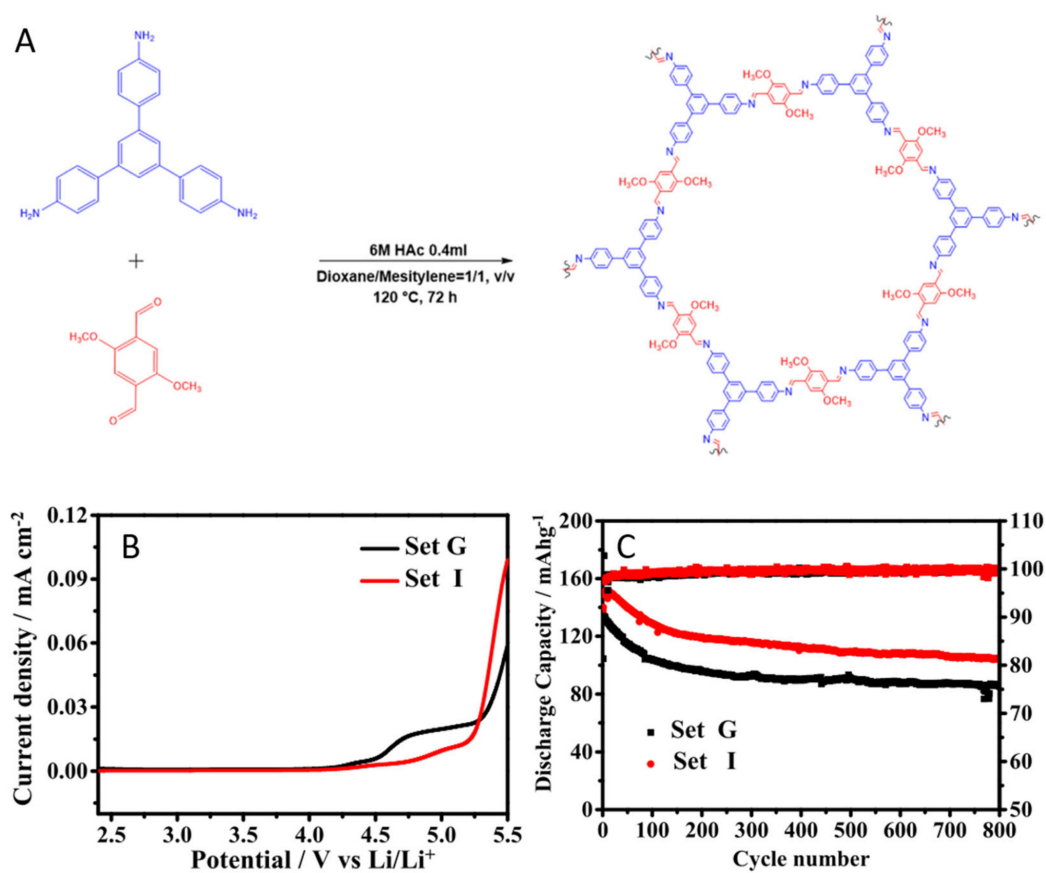


Figure 2. (A) Scheme of TAPB-DMTP-COF preparation; (B) linear scan voltammograms of cells assembled by inserting IGEs between a working stainless-steel electrode and a Li-metal counter electrode at 1 mVs^{-1} . Set G, reference ionic liquid and Set I, ionic liquid with COF; (C) charge/discharge performance of cell $\text{LiFePO}_4 \mid \text{SSE} \mid \text{Li}$ at 60°C . Reprint with permission from [41]. Copyright 2021 American Chemical Society.

Regarding all materials with crystal structures, COFs are not ideal crystals and have some thermodynamically stabilized defects; however, Li and coworkers studied this even further [43]. Their idea was to intentionally induce defects using some part of 2,5-dihydroxybenzaldehyde (DHA) instead of 2,5-dihydroxyterephthalaldehyde (DHTA) (Figure 3). The reaction between TAPB (which was used as a crosslinker) and DHA (with one aldehyde group) resulted in an incomplete closed COF structure. The post-functionalization process contained anchoring ionic groups on defects via Schiff-base reaction with 3-benzyl-2-formyl-1-methyl-1H-imidazol-3-ium bromide. The next step was ionic exchange of bromine to Li cation, from LITSFI source. As an effect of these operations, a COF with a flexible cationic active site was fabricated and the optimized DHA/DHTA ratio was 3/2. Even at the high ratio of unconnected linkers, the samples presented high crystallinity, and the FTIR measurements showed an increase in the NH_2 absorbance signal. The obtained material presented ionic conductivity of $9.74 \times 10^{-5} \text{ S}\cdot\text{cm}^{-1}$ at 30°C , and the material showed unusual stability up to 5.23 V vs. $\text{Li} \mid \text{Li}^+$. The authors prepared a solid-state battery setup with a lithium metal anode and a LiFePO_4 cathode which had $143 \text{ mAh}\cdot\text{g}^{-1}_{\text{cathode}}$ capacity over 40 cycles at 0.1 C, at 80°C . It is worth mentioning that this temperature cannot be used in a commercial liquid electrolyte.

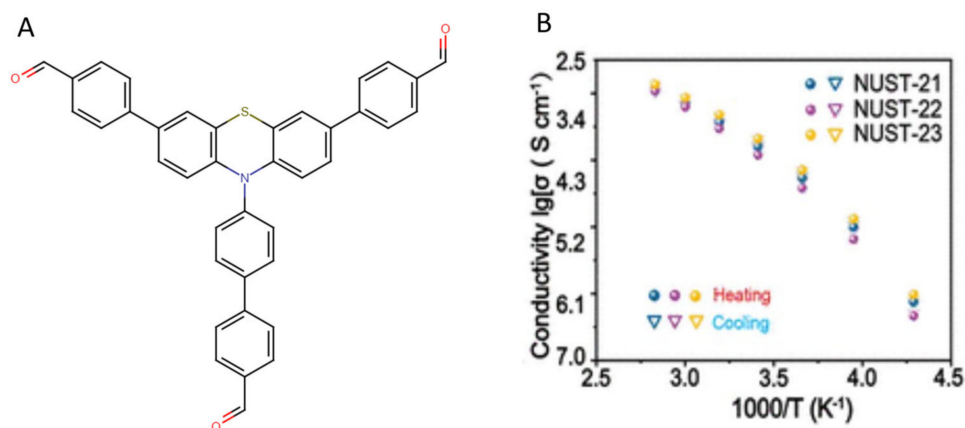


Figure 3. (A) Chemical structure of sulfur-bridged tris(4'-carboxy-1,1'-biphenyl)amine as aldehyde compound for COF synthesis; (B) conductivity of prepared samples: 21 samples contain TAPB linker, 22 samples contain TAPA, 23 samples contain TAPT. Reprinted with permission from [41]. Copyright 2022 American Chemical Society.

One of the issues for a liquid-based electrolyte battery is its very poor performance at temperatures below 0 °C, which is very important, especially for electric vehicles working in winter seasons [44]. One of the solutions proposed by Xuan et al. [45] adopted C₃-symmetric amines (TAPA (tris(4-aminophenyl)amine), TAPB (1,3,5-tris(4-aminophenyl)benzene), and TAPT (4,4',4''-(1,3,5-triazine-2,4,6-triyl)trianiline)) and sulfur-bridged tris(4'-carboxy-1,1'-biphenyl)amine, named as PT-CHO (Figure 4).

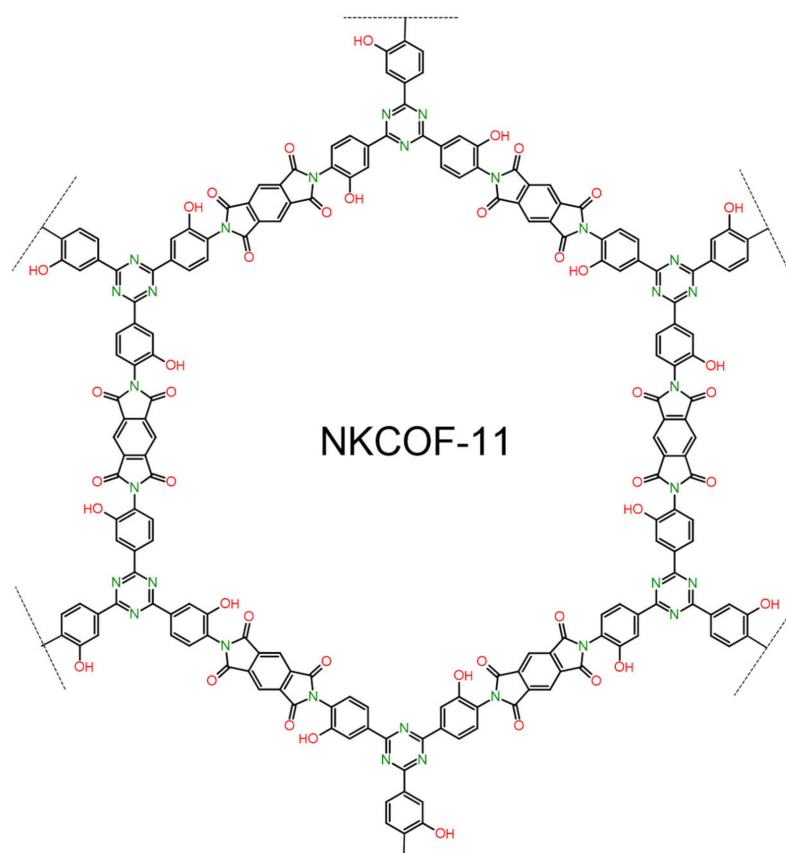


Figure 4. Schematic representation of NKCOF-11 material, adapted from [46].

For the electrochemical measurements, pores of the prepared materials were filled with PEG250 chains and LiTFSI salt. The TAPT-PT-CHO sample presented interesting Li

transport properties: at $-40\text{ }^{\circ}\text{C}$, it presented $9.7 \times 10^{-7}\text{ S}\cdot\text{cm}^{-1}$, and at $20\text{ }^{\circ}\text{C}$, it increased to $2.08 \times 10^{-4}\text{ S}\cdot\text{cm}^{-1}$. The materials presented high stability working with a symmetrical Li electrode, LiFePO_4 cathode, and Li metal anode at low temperatures.

Imine-bonded COF materials hold significant prominence among all COF-based electrolytes. These materials exhibit a notably high transference number of 0.93 and impressive conductivity of $7.2 \times 10^{-3}\text{ S}\cdot\text{cm}^{-1}$ [39]. A layer of this type of COF can also prevent Li dendrite growth during the charging/discharging process [38]. In other studies, researchers have demonstrated the efficient functionality of their imine-bonded materials at elevated temperatures [43] as well as at low temperatures ($-40\text{ }^{\circ}\text{C}$) [44]. The utilization of imine-bonded COF materials presents an interesting proposition for solid-state electrolytes.

2.1.2. Imide Bond

One of the other described C-N systems is the imide bond. Polyimide polymers are well known for their good thermal stability, chemical resistance, and great mechanical properties. Imide bond-linked COFs are formed from the condensation reaction of aromatic anhydride and C_3 -symmetric aromatic primary amine through the formation of aromatic amic acid as an intermediate, and depending on the substrate structure, the formed COFs have hexagonal, square, or triangular shape pores.

Imide bonds have significant thermal stability which was shown in the publication from Wang et al. [46]. Their COF-based material was constructed with pyromellitic dianhydride (PMDA) and 2,4,6-tris(2-aminophenyl)-1,3,5-triazine (TAPOA) at $180\text{ }^{\circ}\text{C}$ for 5 days in the presence of isoquinoline as a catalyst in a mesitylene/NMP mixed solution. The obtained material, denoted as NKCOF-11 (Figure 4), showed imide bonding and high crystallinity. The authors conducted an in-depth study on the behavior of NKCOF-11 at high temperatures. Up to around $350\text{ }^{\circ}\text{C}$, the basic structure remained unchanged, but a thermally induced structural rearrangement from the imide- to the benzoxazole-linked COF (named TR-NKCOF-11) occurred around $400\text{ }^{\circ}\text{C}$, and more carbonization occurred above $650\text{ }^{\circ}\text{C}$. Compared to other COF-based materials (boronate ester, imine, imide, β -ketoenamine, and olefin, details in [46]), NKCOF-11 showed remarkable resistance with respect to a fire test. In order to enhance conductivity, PEG chains and LiTFSI salt were incorporated into the pores of both samples. NKCOF-11 showed good Li-ion conductivity specified as $1.36 \times 10^{-5}\text{ S}\cdot\text{cm}^{-1}$ at $30\text{ }^{\circ}\text{C}$, low energy activation of 0.18 eV, with almost pure ionic conductivity (the transference number was 0.95). TR-NKCOF-11 prepared in the same way showed a lower conductivity value specified as $2.24 \times 10^{-6}\text{ S}\cdot\text{cm}^{-1}$ at $30\text{ }^{\circ}\text{C}$. It is worth mentioning that NKCOF-11 represented impressive electrochemical stability up to 5.5 V vs. $\text{Li}|\text{Li}^+$, which was compatible with state-of-the-art cathode materials like LiNiPO_4 olivine [47].

Jagt et al. [48] prepared a polyimide COF that was based on aromatic triamines: tris(4-aminophenyl)amine (TAPA), 1,3,5-tris(4-aminophenyl)benzene (TAPB), and aromatic dianhydrides (pyromellitic dianhydride (PMDA) or 1,4,5,8-naphthalenetetracarboxylic dianhydride (NTCDA)). They used the solvothermal synthesis method, and used the mixed solvents of NMP and meta-cresol in the presence of isoquinoline as the catalyst. All the compositions had large surface areas of $600\sim 1400\text{ m}^2\text{ g}^{-1}$ and featured high CO_2 capacity of $50\sim 66\text{ cm}^3\text{ g}^{-1}$ at 1.2 bar, thermal stability up to around $500\sim 550\text{ }^{\circ}\text{C}$, and excellent chemical stability to 1 M NaClO_4 @EC/DEC and 1 M Na_2SO_4 @ H_2O . The COF material had excellent chemical stability to 1 M NaClO_4 @EC/DEC and 1 M Na. Unfortunately, they did not measure ionic conductivity and transference number, so their samples could not be completely characterized as SSE. This research included information about reduction potentials versus $\text{Na}|\text{Na}^+$ and $\text{Li}|\text{Li}^+$. On the one hand, COFs with PMDA blocks had around 1.9 V vs. $\text{Li}|\text{Li}^+$ and around 1.5 V vs. $\text{Na}|\text{Na}^+$. On the other hand, those with NTCDA blocks had around 2.5 V vs. $\text{Li}|\text{Li}^+$ and around 2.2 V vs. $\text{Na}|\text{Na}^+$. This result indicated the impact of conjugated aromatic rings on the redox behavior of COF materials (Figure 5).

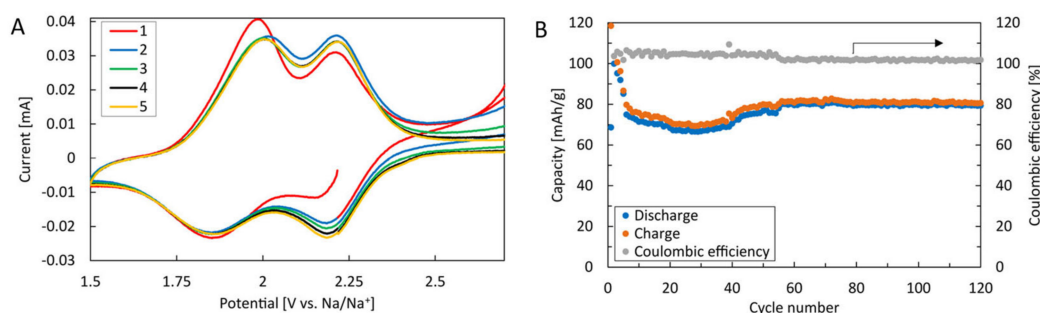


Figure 5. Electrochemical performance of a TAPA-NTXDA system in sodium ion batteries: (A) Cyclic voltammogram with a scan rate of 0.1 mV s^{-1} ; (B) cyclic performance at a rate of 0.1 C (15 mA g^{-1}). Reproduced from reference [48] (CC-BY-NC-ND).

Imide-bonded materials exhibit enhanced electrochemical behavior and are more frequently employed as electrode materials in batteries. Nevertheless, their remarkable chemical and thermal stability can offset the typically lower conductivities. This type of material requires further investigations.

2.1.3. β -Ketoenamine Bond

Jeong et al. proposed an interesting method of increasing ionic conductivity in a β -ketoenamine COF system [49]. As a standard method of preparation, the COF as SSEs contained both Li salt and solvent, as described in previous subsections. The building blocks with cationic active centers dissolved Li salt without any solvent. The prepared COF was constructed with 1,3,5-triformylphloroglucinol (TP) and 1,4-phenylenediamine-2-sulfonic acid (Pa-SO₃H). TpPa-SO₃Li was obtained through ionic exchange using lithium acetate. TpPa-SO₃Li showed relatively small pores of 11.8 \AA and a small surface area of $348 \text{ m}^2 \text{ g}^{-1}$, with a conductivity of $2.7 \times 10^{-5} \text{ S}\cdot\text{cm}^{-1}$, a high transference number of 0.9, and low activation energy equal to 0.18 eV . TpPa-SO₃Li displayed excellent stability with the symmetrical Li cell Li | TpPa-SO₃Li | Li. The DFT calculations represented anisotropy in the conduction direction, low energy ($7.6 \text{ kcal}\cdot\text{mol}^{-1}$) in the axial pathway, and high energy in the planar direction ($31.6 \text{ kcal}\cdot\text{mol}^{-1}$).

Cheng et al. demonstrated that polyethylene oxide assisted Li-ion conductivity inside a COF [50]. They designed and synthesized ketoenamine COFs (TPBD) composed of Tp and benzidine (BD) building blocks, and LiPF₆ salt was utilized as a lithium-ion donor. The -C=O site in TPBD provided stronger integration on Li⁺ than the unketoned form from the imine-linked COF (TFBD) composed of 1,3,5-benzene tricarboxaldehyde (TF) and BD, which enhanced the dissociation of LiPF₆. The ketoenamine TPBD provided a -NH group that formed a hydrogen bond with PF₆ and increased t_{Li^+} , i.e., the conductivity was $3.14 \times 10^{-6} \text{ S}\cdot\text{cm}^{-1}$ at $25 \text{ }^\circ\text{C}$, the transference number was $t_{\text{Li}^+} = 0.724$, and the high activation energy was 0.84 eV . Embedding of TPBD-LiPF₆ in PEO provided two orders of magnitude higher lithium-ion conductivity to $5.43 \times 10^{-4} \text{ S}\cdot\text{cm}^{-1}$ at $25 \text{ }^\circ\text{C}$, and the activation energy was equal to 0.37 eV ; however, the transference number was 0.455. TPBD-LiPF₆@PEO had stable electrochemical operation as large as 4.2 V (vs. Li⁺/Li) in the cell setup with lithium and stainless-steel electrodes on each side. The LiFePO₄ | TPBD-LiPF₆@PEO | Li battery assembled without the use of a liquid electrolyte showed a specific capacity of almost 140 mAh g^{-1} at 0.2 C and a Coulombic efficiency of 99.6% after 200 cycles at $25 \text{ }^\circ\text{C}$.

β -Ketoenamine-linked covalent organic frameworks (COFs) offer excellent structural versatility and outstanding aqueous stability, but their stability complicates obtaining samples with high crystallinity and surface area. The presented examples show the possibility of applying this type of material as a solid electrolyte due to its good transference number and stability that cover moderate-voltage cathode materials. Its conductivities still can be improved.

2.1.4. Squaraine Linkage

A squaramide is one of the squaraine-type linkages that is composed of both zwitterionic and amide bonds via the condensation reaction of aromatic amines and squaric acid. Squaraines that contain squaramide exhibit appealing characteristics such as strong infrared absorption and photostability, which have been extensively described in previous studies [51,52]. Wang et al. investigated the utilization of a squaraine-linked covalent organic framework (COF) (Figure 6) as an additive for a polyethylene oxide (PEO)-based electrolyte [53]. The COF, named HUT4, was synthesized by reacting melamine and squaric acid at 120 °C for 3 days. The resulting material exhibited a pore size of 15 Å and a surface area of 120 m² g⁻¹. They developed a hybrid electrolyte by embedding HUT4 in PEO and combining it with the lithium donor LiTFSI. Among the different compositions tested, the electrolyte with 10% HUT4 additive demonstrated the best performance, leading to good ionic conductivity of 8.2×10^{-6} S·cm⁻¹ at 30 °C, regardless of a moderate transference number of 0.62. This performance was nearly twice as good as that of the sample without the addition of HUT4. To further evaluate the applicability of this material, the authors assembled a S@CNT|PEO-10%HUT4|Li cell. Under operating conditions of 60 °C and a current rate of 0.2 C, the cell exhibited a capacity of approximately 1000 mAh g⁻¹, demonstrating the potential application of this material in Li-S batteries. Although this type of bonding has theoretically shown significant potential, it has not yet been properly explored.

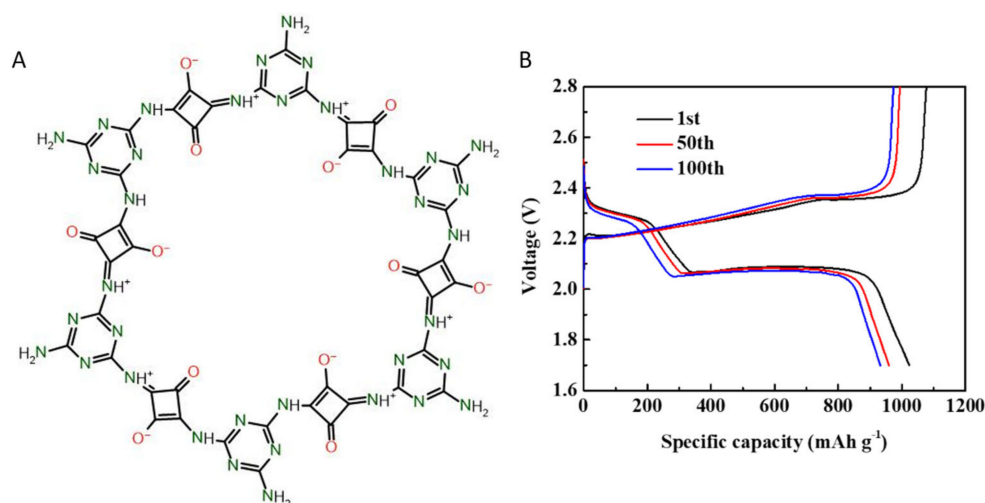


Figure 6. (A) HUT4 sample, reproduced from [53]; (B) charge/discharge curves of cell S@CNT|PEO-10%HUT4|Li. Reprint with permission from [53]. Copyright 2022 American Chemical Society.

The presence of ionic-type bonding in squaraine-type COF materials positions them as promising candidates for lithium-ion conductors. However, it is important to note that the strong electrostatic interactions between ions and structure raise the activation energy required for ion movement, potentially leading to reduced conductivity, as illustrated earlier. Nevertheless, their stable performance in Li-S batteries suggests that this material category holds significant potential and merits further comprehensive investigation.

2.1.5. Triazine Linkage

The triazine linkage is a chemical connection utilized in the construction of COFs that entail the bonding of nitrogen atoms within triazine rings. This linkage significantly contributes to the structural integrity and stability of the structure. Triazine-linked COFs have garnered significant interest, primarily owing to their remarkable thermal stability. Cheng et al. [54] presented an interesting example of a COF material with triazine-type bonds, which was synthesized by the condensation reaction of triazine and piperazine rings (NCS) (Figure 7). The loose bonding between the triazine rings and cations reduced the energy barrier during ion transfer, which allowed for efficient movement of lithium

ions. Additionally, the electrostatic forces with the piperazine rings acted as anchors, enhancing the selectivity of ion transfer by effectively binding anions. As a result, the NCS/electrolyte demonstrated exceptional room temperature lithium-ion conductivity, reaching up to $1.49 \times 10^{-3} \text{ S}\cdot\text{cm}^{-1}$. This conductivity was achieved without the need for any solvent, only with the addition of LiTFSI, making it a promising and environmentally friendly option. Furthermore, the NCS/electrolyte exhibited a high transference number of 0.84, indicating efficient lithium-ion transport with minimal interference from other ions.

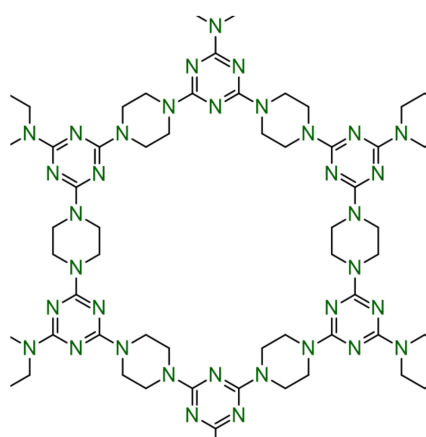


Figure 7. COF structure based on triazine and piperazine rings. Adapted from [54].

The example presented demonstrated a triazine-bonded material with significant promise as an electrolyte for solid-state batteries (SSB). This material exhibited high conductivity coupled with a favorable transference number. Its noteworthy characteristic of being devoid of oxygen contributed to enhanced thermal stability, although this aspect was not quantified in the study. However, further extensive research is warranted to explore the full potential of such materials.

2.2. C-B and O-B Linkages

In addition to the various types of chemical bonding found in covalent organic frameworks (COFs), carbon-boron (C-B) and oxygen-boron (O-B) linkages have emerged as noteworthy bonding motifs. COFs that incorporate C-B and O-B bonds have attracted considerable attention due to their unique properties and potential applications across diverse fields. The introduction of boron atoms into COF structures has brought about new functionalities and characteristics that could be tailored for specific purposes. COFs with oxygen-boron bonds, such as boronic acids and boroxinates, possess intriguing properties associated with their acidic nature and unique electronic structure. The presence of oxygen atoms in the boron-containing linkages facilitates proton transfer and acid–base interactions, rendering them potential candidates for proton-conducting materials, sensors, and drug delivery systems. Furthermore, the integration of oxygen-boron bonds within COFs imparts advantageous optical and electronic characteristics, thereby opening avenues for deployment in optoelectronic devices, photovoltaic systems, and as demonstrated in the following illustrative instances, as an electrolyte.

2.2.1. Spiroborate Bond

The spiroborate bond in COFs is a unique structural element where boron atoms form a closed ring with neighboring oxygen atoms, creating a stable and versatile linkage. This bond plays a crucial role in enhancing COF stability and enabling various applications, particularly in the field of battery electrolytes, due to its excellent ion-conducting properties. A good example is the works by Du et al. presented in [55]. Figure 8 shows the structure of high crystalline spiroborate-based COFs described as ICOF-2.

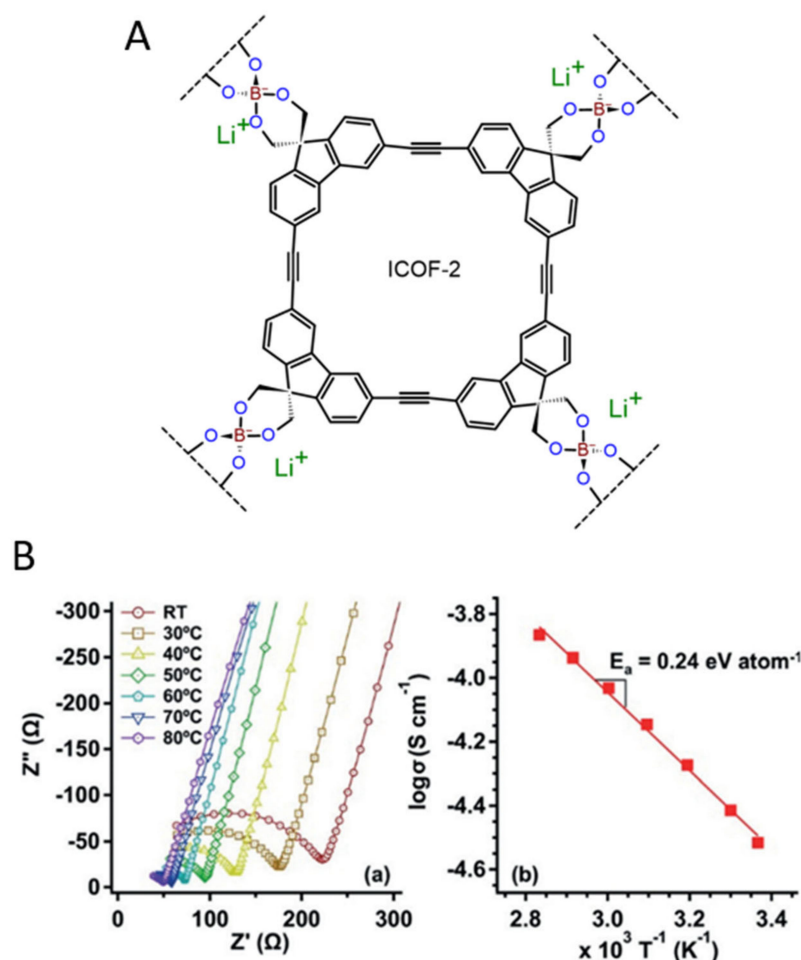


Figure 8. (A) Scheme of ICOF-2 structure; (B) Nyquist and Arrhenius type plots of ICOF-2 reproduction, with permission from [55]. Copyright 2016, Wiley-VCH.

All the COFs showed high crystalline two-dimensional structures ordered in A-A or A-B stacking. The boronate ester linkage contained sp^3 -hybridized boron which formed an ionic linkage. The presence of anionic boron centers in spiroborate-based COFs created possible routes for high conductivity paths. Therefore, the conductivities of ICOF-1 and ICOF-2 showed high porosities of $1022 \text{ m}^2 \text{ g}^{-1}$ and $1259 \text{ m}^2 \text{ g}^{-1}$, respectively, and they also possessed high thermal stability (mass loss up to 20% at 800°C on TG measurement) and chemical stability vs. LiOH solution in water. Lithium ions were incorporated using LiOH (ICOF-2) instead of dimethyl amine base solution (ICOF-1) during COF formation. The conductivity of ICOF-2 was activated with an activation energy of 0.24 eV and moderate ionic conductivity of $3.05 \times 10^{-5} \text{ S}\cdot\text{cm}^{-1}$ at room temperature. The transference number determined by the Bruce–Vincent–Evans method was 0.8. Among other properties, the high H_2 and CH_4 uptakes of ICOF-1 and ICOF-2 were of great worth as 3.11 \%_w at 77 K (1 bar) and 4.62 \%_w at 273 K (1 bar), respectively. Another advantage of the prepared materials was significant hydrolysis resistance. The authors' strategy of spiroborate formation provided the possibility of preparing porous materials with moderate electrolyte properties.

Other spiroborate COFs have also been reported by Zhang et al. [27], which were prepared from the reaction of γ -cyclodextrin and trimethyl borate with respective counter ions such as Li^+ , piperazine, and dimethyl amine (CD-COF-Li, CD-COF-PPZ, and CD-COF-DMA) using the microwave-assisted solvothermal synthesis method. The cyclodextrine-based COF presented a robust skeleton with a high specific area of $760 \text{ m}^2\cdot\text{g}^{-1}$. CD-COF-Li after loading with a standard liquid electrolyte (LiPF_6 in EC/DEC) showed remarkable Li^+ conductivity of $2.7 \times 10^{-3} \text{ S}\cdot\text{cm}^{-1}$ at 30°C . The rapid Li^+ transportation could be attributed to the flexible nature of γ -cyclodextrin, high porosity, and anionic nature of the

spiroborate linkage. These spiroborate-linked COFs with γ -cyclodextrin also showed stable performance when cycling in a cell with symmetrical lithium metal electrodes. Interestingly, CD-COF-Li had high CO_2/N_2 sorption/desorption selectivity, which confirmed that this COF material was suitable for gas separation membranes.

The showcased examples demonstrate the potential of spiroborate-linked COF materials as viable electrolytes, attributed to their capacity for achieving high Li^+ conductivity and impressive thermal stability. Moreover, the exceptional surface area of these materials opens up opportunities for their utilization in various other applications beyond electrolytes.

2.2.2. Boronate Ester

Boronic ester bonds, often referred to as boronate ester bonds, are a class of covalent bonds that involve boron atoms. These bonds are formed through the reaction between a boronic acid group and an alcohol group, resulting in the formation of a stable covalent linkage. Boronic ester bonds are highly valued in COF chemistry because of their reversible nature. They can undergo dynamic covalent chemistry, allowing for the disassembly and reassembly of COF structures under certain conditions. This reversibility makes boronic ester-linked COFs promising candidates for applications such as drug delivery systems, sensors, and molecular recognition, where controlled release or selective binding is required. In the realm of electrolyte applications, a paucity of research papers has explored the utilization of this specific bond type, with one notable exemplar presented below.

Vazquez-Molina et al. [56] described another interesting aspect of COF materials. In general, materials obtained by solvothermal reactions and other processes have polycrystalline aggregate structures. Chaotic crystal ordering leads to discontinuities in the optimal Li^+ pathway, resulting in higher activation energies for Li^+ transport and lower conductivity. The authors ordered the crystal grains of a boronate-bonded COF, described in the literature as COF-5, by applying uniaxial pressure. They used pressure in the range of 2–12 MPa, but the ordering of layers could be observed from 2 MPa, and a further increase in the pressure did not change the XRD pattern significantly. For the electrochemical measurements, the sample COF-5 was prepared by incorporating 1 M LiClO_4 in THF. The conductivity reached $2.6 \times 10^{-4} \text{ S}\cdot\text{cm}^{-1}$, but the authors did not specify the influence of the used pressure on the conductivity. The sample also presented extraordinary stability from -1 to 10 V vs. $\text{Li}^+|\text{Li}$ in the $\text{Li}|\text{LiClO}_5@\text{COF-5}|\text{Li}$ cell setup. The high ionic conductivity, low temperature effect on conductivity, and high electrochemical stability makes crystallographically aligned COF-5 a competitive candidate for solid electrolytes in rechargeable Li-ion batteries.

The existing literature offers only a limited number of instances concerning boronate ester bonds in COFs. The provided example in [56] demonstrated a straightforward and efficient method for producing textured COF-5 with substantial conductivity. However, further comprehensive investigations are warranted to explore the full potential of these materials.

3. Conclusions, Challenges, and Future Directions

As previously discussed, covalent organic frameworks (COFs) show immense potential as a foundational element for solid-state batteries. Even though scientists worldwide have significantly contributed to COF materials cognition, substantial potential for refinement persists. There remains considerable room for refining their functional properties. When contrasted with conventional polymer separators such as PEO and PC, COFs showcase heightened conductivity due to different molecular structures, rendering them viable across a wider temperature spectrum than liquid and polymer electrolytes with conductivities higher than typical polymer electrolytes (as evidenced in Table 1). Furthermore, they boast escalated thermal and electrochemical stability, along with greater elasticity compared to most inorganic solid electrolytes. Nevertheless, several frontiers beckon further exploration and comprehension to optimize COF performance as follows:

- Building blocks and pore structure Investigating the type of building blocks used and understanding the impact on the 2D or 3D pore structures of COFs is crucial for optimizing charge mobility within the material.
- Structure stiffness Balancing the degree of structure stiffness is important, as more rigid structures can impede ion mobility, while excessively flexible structures can compromise mechanical integrity.
- Ionic character Exploring the presence of active centers (anionic, cationic, mixed, or neutral) within COFs can aid in the dissolving of lithium salts, which are important for ion conduction.
- Li donor The selection of suitable lithium salts, such as LiPF₆, LiClO₄, LiTFSI, is crucial for facilitating ion transport within the COF structure.
- Plasticizers and fillers Understanding the influence of plasticizers and fillers on Li⁺ mobility is important. Ideally, COF materials should possess intrinsic conductivity without the need for additional plasticizers.
- Solvents Delving into the role of solvents in the dissociation of lithium donors can provide insights into improving ion conductivity within COF electrolytes.

Table 1. Comparison of the most important electrolyte parameters between different COF linkages.

Type of Bond	Linkers	σ_{Li^+}	Li ⁺ Transference Number; Stability vs. Li ⁺ Li	Ref.
Squaraine	-Squaric acid -Melamine	8.2×10^{-6} S/cm @30 °C	0.62; -	[53]
Triazine	-Triazine -Piperazine	1.49×10^{-3} S/cm @RT	0.84; -	[54]
Imine	-Trisfromylbenzene -Fluorinated-imidazole containing diamine (see Figure 1)	7.2×10^{-3} S/cm @RT	0.81; 0–4.5 V	[39]
Imine	-Trisfromylbenzene -Diaminobenzene	-	0.85; Stable near 0 V	[38]
Imine	-2,4,6-Tris(4-aminophenyl)-1,3,5-triazine -2,3,5,6-Tetrafluoroterephthalaldehyde	5.3×10^{-3} S/cm @30 °C	-; up to 5.6 V	[40]
Imine	-Tri(4-aminophenyl)benzene -Dimethoxyterephthalaldehyde	2.8×10^{-4} S/cm @30 °C	-	[41]
Imine	-3,5-Bis(5-formylthiophen-2-yl)phenyl]thiophene-2-carbaldehyde -Tri(4-aminophenyl)amine	2.2×10^{-4} S/cm @40 °C	-; up to 3.4 V	[42]
Imine	-2,5-Dihydroxybenzaldehyde -Tri(4-aminophenyl)benzene	9.74×10^{-5} S/cm @30°C	-; up to 5.5 V	[43]
Imide	-2,4,6-Tris(2-aminophenyl)-triazine -Pyromellitic dianhydride	1.36×10^{-5} S/cm @30 °C	0.95; up to 5.5 V	[46]
β -Ketoenamine	-Triformylphloroglucinol -Benzidine	2.14×10^{-4} S·cm ⁻¹ @25 °C	0.724; -	[50]
β -Ketoenamine	-1,4-Phenylenediamine-2-sulfonic acid -Triformylphloroglucinol	2.7×10^{-7} S·cm ⁻¹ @RT	0.9; -	[49]
Boronate ester	-Benzene dibornic acid -Hexahydroxytriphenylene	2.6×10^{-4} S·cm ⁻¹ @25 °C	-; –1–10 V	[56]
Spiroborate	-Trimethyl borate -3,6-Di(prop-1-yn-1-yl)-9H-fluorene-9,9-dicarboxylate	3.05×10^{-5} S/cm @RT	0.8; -	[55]
Spiroborate	-Trimethyl borate - γ -Cyclodextrin	2.7×10^{-3} S/cm @RT	-	[27]

Navigating the intricate landscape of COF-based electrolytes demands a holistic grasp of challenges, innovative remedies, and trajectories for future inquiry. The COF-based electrolytes introduce numerous challenges, prompting the optimization of building block selection for desired properties, all the while ensuring structural stability—requiring meticulous design guided by a profound understanding of material behavior. The delicate balance between structural rigidity and ion mobility necessitates inventive approaches. Deciphering the optimal ionic character and addressing the complex interplay of anionic, cationic, mixed, or neutral centers assumes paramount importance for enhanced ion conduction. Surmounting these multifaceted challenges mandates a multidisciplinary approach. Leveraging advanced material design intertwined with molecular engineering principles bears the promise of yielding novel COF structures tailored for specific applications. The fusion of experimental techniques and computational simulations opens a window into the nuances of COF behavior, enabling performance prediction. Collaboration across the disciplines of materials science, chemistry, physics, and engineering is pivotal in surmounting these obstacles.

In conclusion, propelling COF materials for solid-state batteries mandates prioritizing the amelioration of key parameters like conductivity, electrochemical stability, and transference number. These attributes hold particular significance for high-power applications, such as electric vehicles. Furthermore, the electrolyte must exhibit electrochemical stability to seamlessly accommodate novel high-voltage cathode materials bearing matching HOMO-LUMO levels. Attaining a transference number nearing unity remains pivotal to mitigate self-discharge concerns, and the stability of COF electrolytes concerning electrode materials assumes critical significance. Moreover, the acknowledgment of the constraints of lithium resources is imperative, kindling exploration into alternative ions like Na⁺ [57], K⁺ [58], Mg²⁺ [59], Al³⁺ [60], Zn²⁺ [12,61], and others, can not only reduce production costs but can also enable the transition away from fossil fuels in transportation and make large-scale energy storage more affordable. As COF materials unveil a promising platform for next-generation batteries, they beckon researchers toward an exciting journey through expanded ion chemistries, paving the path for a more ecologically sustainable energy landscape.

Author Contributions: Conceptualization, T.P.; writing—original draft preparation, T.P.; writing—review and editing, T.P. and A.N.; supervision, A.N. All authors have read and agreed to the published version of the manuscript.

Funding: This research was funded by the International Research Agendas programme of the Foundation for Polish Science, co-financed by the European Union under the European Regional Development Fund and the European Union's Horizon 2020, (grant number GA No. MAB/2020/14).

Data Availability Statement: Not applicable.

Conflicts of Interest: The authors declare no conflict of interest.

References

1. Koohi-Fayegh, S.; Rosen, M. A review of energy storage types, applications and recent developments. *J. Energy Storage* **2020**, *27*, 101047. [[CrossRef](#)]
2. Xiao, J.; Li, H.; Zhang, H.; He, S.; Zhang, Q.; Liu, K.; Jiang, S.; Duan, G.; Zhang, K. Nanocellulose and its derived composite electrodes toward supercapacitors: Fabrication, properties, and challenges. *J. Bioresour. Bioprod.* **2022**, *7*, 245–269. [[CrossRef](#)]
3. Hassan, Q.; Sameen, A.Z.; Salman, H.M.; Jaszczur, M.; Al-Jiboory, A.K. Hydrogen energy future: Advancements in storage technologies and implications for sustainability. *J. Energy Storage* **2023**, *72*, 108404. [[CrossRef](#)]
4. Masias, A.; Marcicki, J.; Paxton, W.A. Opportunities and Challenges of Lithium Ion Batteries in Automotive Applications. *ACS Energy Lett.* **2021**, *6*, 621–630. [[CrossRef](#)]
5. Nzereogu, P.; Omah, A.; Ezema, F.; Iwuoha, E.; Nwanya, A. Anode materials for lithium-ion batteries: A review. *Appl. Surf. Sci. Adv.* **2022**, *9*, 100233. [[CrossRef](#)]
6. Li, D.; Guo, H.; Jiang, S.; Zeng, G.; Zhou, W.; Li, Z. Microstructures and electrochemical performances of TiO₂-coated Mg–Zr co-doped NCM as a cathode material for lithium-ion batteries with high power and long circular life. *New J. Chem.* **2021**, *45*, 19446–19455. [[CrossRef](#)]

7. Jayalakshmi, T.; Harini, R.; Nagaraju, G. Lithium ion battery performance of micro and nano-size V₂O₅ cathode materials. *Mater. Today Proc.* **2022**, *65*, 200–206. [[CrossRef](#)]
8. Blomgren, G.E. The Development and Future of Lithium Ion Batteries. *J. Electrochem. Soc.* **2017**, *164*, A5019–A5025. [[CrossRef](#)]
9. Kim, T.; Song, W.; Son, D.-Y.; Ono, L.K.; Qi, Y. Lithium-ion batteries: Outlook on present, future, and hybridized technologies. *J. Mater. Chem. A* **2019**, *7*, 2942–2964. [[CrossRef](#)]
10. Tian, Y.; Zeng, G.; Rutt, A.; Shi, T.; Kim, H.; Wang, J.; Koettgen, J.; Sun, Y.; Ouyang, B.; Chen, T.; et al. Promises and Challenges of Next-Generation “Beyond Li-ion” Batteries for Electric Vehicles and Grid Decarbonization. *Chem. Rev.* **2021**, *121*, 1623–1669. [[CrossRef](#)]
11. Janek, J.; Zeier, W.G. A solid future for battery development. *Nat. Energy* **2016**, *1*, 16141. [[CrossRef](#)]
12. Deng, W.; Xu, Y.; Zhang, X.; Li, C.; Liu, Y.; Xiang, K.; Chen, H. (NH₄)₂Co₂V₁₀O₂₈·16H₂O/(NH₄)₂V₁₀O₂₅·8H₂O heterostructure as cathode for high-performance aqueous Zn-ion batteries. *J. Alloys Compd.* **2022**, *903*, 163824. [[CrossRef](#)]
13. Zhou, G.; Chen, H.; Cui, Y. Formulating energy density for designing practical lithium–sulfur batteries. *Nat. Energy* **2022**, *7*, 312–319. [[CrossRef](#)]
14. Yang, Y.; Hong, X.-J.; Song, C.-L.; Li, G.-H.; Zheng, Y.-X.; Zhou, D.-D.; Zhang, M.; Cai, Y.-P.; Wang, H. Lithium bis(trifluoromethanesulfonyl)imide assisted dual-functional separator coating materials based on covalent organic frameworks for high-performance lithium–selenium sulfide batteries. *J. Mater. Chem. A* **2019**, *7*, 16323–16329. [[CrossRef](#)]
15. Deng, W.-N.; Li, Y.-H.; Xu, D.-F.; Zhou, W.; Xiang, K.-X.; Chen, H. Three-dimensional hierarchically porous nitrogen-doped carbon from water hyacinth as selenium host for high-performance lithium–selenium batteries. *Rare Met.* **2022**, *41*, 3432–3445. [[CrossRef](#)]
16. Tian, H.; Tian, H.; Wang, S.; Chen, S.; Zhang, F.; Song, L.; Liu, H.; Liu, J.; Wang, G. High-power lithium–selenium batteries enabled by atomic cobalt electrocatalyst in hollow carbon cathode. *Nat. Commun.* **2020**, *11*, 5025. [[CrossRef](#)] [[PubMed](#)]
17. McDonagh, A.M.; Tkacheva, A.; Sun, B.; Zhang, J.; Wang, G. Nitronyl nitroxide-based redox mediators for Li-O₂ batteries. *J. Phys. Chem. C* **2021**, *125*, 2824–2830. [[CrossRef](#)]
18. Kamaya, N.; Homma, K.; Yamakawa, Y.; Hirayama, M.; Kanno, R.; Yonemura, M.; Kamiyama, T.; Kato, Y.; Hama, S.; Kawamoto, K.; et al. A lithium superionic conductor. *Nat. Mater.* **2011**, *10*, 682–686. [[CrossRef](#)] [[PubMed](#)]
19. Hayamizu, K.; Seki, S.; Haishi, T. 7Li NMR diffusion studies in micrometre-space for perovskite-type Li_{0.33}La_{0.55}TiO₃ (LLTO) influenced by grain boundaries. *Solid State Ion.* **2018**, *326*, 37–47. [[CrossRef](#)]
20. Polczyk, T.; Zając, W.; Ziabka, M.; Świerczek, K. Mitigation of grain boundary resistance in La_{2/3-x}Li_{3x}TiO₃ perovskite as an electrolyte for solid-state Li-ion batteries. *J. Mater. Sci.* **2020**, *56*, 2435–2450. [[CrossRef](#)]
21. Wu, J.-F.; Guo, X. Size effect in nanocrystalline lithium-ion conducting perovskite: Li_{0.30}La_{0.57}TiO₃. *Solid State Ion.* **2017**, *310*, 38–43. [[CrossRef](#)]
22. Xu, S.; Hu, L. Towards a high-performance garnet-based solid-state Li metal battery: A perspective on recent advances. *J. Power Sources* **2020**, *472*, 228571. [[CrossRef](#)]
23. Zhou, D.; Shanmukaraj, D.; Tkacheva, A.; Armand, M.; Wang, G. Polymer Electrolytes for Lithium-Based Batteries: Advances and Prospects. *Chem* **2019**, *5*, 2326–2352. [[CrossRef](#)]
24. Li, C.; Liu, L.; Kang, J.; Xiao, Y.; Feng, Y.; Cao, F.-F.; Zhang, H. Pristine MOF and COF materials for advanced batteries. *Energy Storage Mater.* **2020**, *31*, 115–134. [[CrossRef](#)]
25. Jiang, S.; Lv, T.; Peng, Y.; Pang, H. MOFs Containing Solid-State Electrolytes for Batteries. *Adv. Sci.* **2023**, *10*, 2206887. [[CrossRef](#)]
26. Wei, T.; Wang, Z.-M.; Zhang, Q.; Zhou, Y.; Sun, C.; Wang, M.; Liu, Y.; Wang, S.; Yu, Z.; Qiu, X.-Y.; et al. Metal–organic framework-based solid-state electrolytes for all solid-state lithium metal batteries: A review. *CrystEngComm* **2022**, *24*, 5014–5030. [[CrossRef](#)]
27. Zhang, Y.; Duan, J.; Ma, D.; Li, P.; Li, S.; Li, H.; Zhou, J.; Ma, X.; Feng, X.; Wang, B. Three-Dimensional Anionic Cyclodextrin-Based Covalent Organic Frameworks. *Angew. Chem. Int. Ed.* **2017**, *56*, 16313–16317. [[CrossRef](#)]
28. Nagai, A.; Guo, Z.; Feng, X.; Jin, S.; Chen, X.; Ding, X.; Jiang, D. Pore surface engineering in covalent organic frameworks. *Nat. Commun.* **2011**, *2*, 536. [[CrossRef](#)] [[PubMed](#)]
29. Fang, Q.; Zhuang, Z.; Gu, S.; Kaspar, R.B.; Zheng, J.; Wang, J.; Qiu, S.; Yan, Y. Designed synthesis of large-pore crystalline polyimide covalent organic frameworks. *Nat. Commun.* **2014**, *5*, 4503. [[CrossRef](#)] [[PubMed](#)]
30. Geng, K.; He, T.; Liu, R.; Dalapati, S.; Tan, K.T.; Li, Z.; Tao, S.; Gong, Y.; Jiang, Q.; Jiang, D. Covalent Organic Frameworks: Design, Synthesis, and Functions. *Chem. Rev.* **2020**, *120*, 8814–8933. [[CrossRef](#)] [[PubMed](#)]
31. Ibrahim, M.; Abdelhamid, H.N.; Abuelftooh, A.M.; Mohamed, S.G.; Wen, Z.; Sun, X. Covalent organic frameworks (COFs)-derived nitrogen-doped carbon/reduced graphene oxide nanocomposite as electrodes materials for supercapacitors. *J. Energy Storage* **2022**, *55*, 105375. [[CrossRef](#)]
32. Dai, Y.; Wang, Y.; Li, X.; Cui, M.; Gao, Y.; Xu, H.; Xu, X. In situ form core-shell carbon nanotube-imide COF composite for high performance negative electrode of pseudocapacitor. *Electrochim. Acta* **2022**, *421*, 140470. [[CrossRef](#)]
33. Nagai, A. *Covalent Organic Frameworks*, 1st ed.; Jenny Stanford Publishing Pte. Ltd.: Singapore, 2020; Volume 1.
34. Gu, S.; Chen, J.; Hao, R.; Chen, X.; Wang, Z.; Hussain, I.; Liu, G.; Liu, K.; Gan, Q.; Li, Z.; et al. Redox of anionic and cationic radical intermediates in a bipolar polyimide COF for high-performance dual-ion organic batteries. *Chem. Eng. J.* **2023**, *454*, 139877. [[CrossRef](#)]

35. Cai, Y.-Q.; Gong, Z.-T.; Rong, Q.; Liu, J.-M.; Yao, L.-F.; Cheng, F.-X.; Liu, J.-J.; Xia, S.-B.; Guo, H. Improved and stable triazine-based covalent organic framework for lithium storage. *Appl. Surf. Sci.* **2022**, *594*, 153481. [[CrossRef](#)]
36. Wu, M.; Zhou, Z. Covalent organic frameworks as electrode materials for rechargeable metal-ion batteries. *Interdiscip. Mater.* **2023**, *2*, 231–259. [[CrossRef](#)]
37. Zeng, S.-M.; Huang, X.-X.; Ma, Y.-J.; Zhi, L.-J. A review of covalent organic framework electrode materials for rechargeable metal-ion batteries. *New Carbon Mater.* **2021**, *36*, 1–18. [[CrossRef](#)]
38. Xu, Y.; Zhou, Y.; Li, T.; Jiang, S.; Qian, X.; Yue, Q.; Kang, Y. Multifunctional covalent organic frameworks for high capacity and dendrite-free lithium metal batteries. *Energy Storage Mater.* **2020**, *25*, 334–341. [[CrossRef](#)]
39. Hu, Y.; Dunlap, N.; Wan, S.; Lu, S.; Huang, S.; Sellinger, I.; Ortiz, M.; Jin, Y.; Lee, S.-H.; Zhang, W. Crystalline Lithium Imidazolate Covalent Organic Frameworks with High Li-Ion Conductivity. *J. Am. Chem. Soc.* **2019**, *141*, 7518–7525. [[CrossRef](#)] [[PubMed](#)]
40. Niu, C.; Luo, W.; Dai, C.; Yu, C.; Xu, Y. High-Voltage-Tolerant Covalent Organic Framework Electrolyte with Holistically Oriented Channels for Solid-State Lithium Metal Batteries with Nickel-Rich Cathodes. *Angew. Chem. Int. Ed.* **2021**, *60*, 24915–24923. [[CrossRef](#)]
41. Wang, Z.; Zheng, W.; Sun, W.; Zhao, L.; Yuan, W. Covalent Organic Frameworks-Enhanced Ionic Conductivity of Polymeric Ionic Liquid-Based Ionic Gel Electrolyte for Lithium Metal Battery. *ACS Appl. Energy Mater.* **2021**, *4*, 2808–2819. [[CrossRef](#)]
42. Shan, Z.; Wu, M.; Du, Y.; Xu, B.; He, B.; Wu, X.; Zhang, G. Covalent organic framework-based electrolytes for fast Li⁺-conduction and high-temperature solid-state lithium-ion batteries. *Chem. Mater.* **2021**, *33*, 5058–5066. [[CrossRef](#)]
43. Li, Z.; Liu, Z.; Li, Z.; Wang, T.; Zhao, F.; Ding, X.; Feng, W.; Han, B. Defective 2D Covalent Organic Frameworks for Postfunctionalization. *Adv. Funct. Mater.* **2020**, *30*, 1909267. [[CrossRef](#)]
44. Steinstraeter, M.; Heinrich, T.; Lienkamp, M. Effect of Low Temperature on Electric Vehicle Range. *World Electr. Veh. J.* **2021**, *12*, 115. [[CrossRef](#)]
45. Xuan, Y.; Wang, Y.; He, B.; Bian, S.; Liu, J.; Xu, B.; Zhang, G. Covalent Organic Framework-Derived Quasi-Solid Electrolyte for Low-Temperature Lithium-Ion Battery. *Chem. Mater.* **2022**, *34*, 9104–9110. [[CrossRef](#)]
46. Wang, Z.; Zhang, Y.; Zhang, P.; Yan, D.; Liu, J.; Chen, Y.; Liu, Q.; Cheng, P.; Zaworotko, M.J.; Zhang, Z. Thermally rearranged covalent organic framework with flame-retardancy as a high safety Li-ion solid electrolyte. *eScience* **2022**, *2*, 311–318. [[CrossRef](#)]
47. Tolganbek, N.; Yerkinbekova, Y.; Kalybekkyzy, S.; Bakenov, Z.; Mentbayeva, A. Current state of high voltage olivine structured LiMPO₄ cathode materials for energy storage applications: A review. *J. Alloys Compd.* **2021**, *882*, 160774. [[CrossRef](#)]
48. Van der Jagt, R.; Vasileiadis, A.; Veldhuizen, H.; Shao, P.; Feng, X.; Ganapathy, S.; Habisreutinger, N.C.; van der Veen, M.A.; Wang, C.; Wagemaker, M.; et al. Synthesis and Structure–Property Relationships of Polyimide Covalent Organic Frameworks for Carbon Dioxide Capture and (Aqueous) Sodium-Ion Batteries. *Chem. Mater.* **2021**, *33*, 818–833. [[CrossRef](#)]
49. Jeong, K.; Park, S.; Jung, G.Y.; Kim, S.H.; Lee, Y.-H.; Kwak, S.K.; Lee, S.-Y. Solvent-Free, Single Lithium-Ion Conducting Covalent Organic Frameworks. *J. Am. Chem. Soc.* **2019**, *141*, 5880–5885. [[CrossRef](#)] [[PubMed](#)]
50. Cheng, D.; Sun, C.; Lang, Z.; Zhang, J.; Hu, A.; Duan, J.; Chen, X.; Zang, H.-Y.; Chen, J.; Zheng, M.; et al. Hybrid covalent organic-framework-based electrolytes for optimizing interface resistance in solid-state lithium-ion batteries. *Cell Rep. Phys. Sci.* **2022**, *3*, 100731. [[CrossRef](#)]
51. Nagai, A.; Chen, X.; Feng, X.; Ding, X.; Guo, Z.; Jiang, D. A Squaraine-Linked Mesoporous Covalent Organic Framework. *Angew. Chem. Int. Ed.* **2013**, *52*, 3770–3774. [[CrossRef](#)] [[PubMed](#)]
52. Qiao, W.; Li, Z. Recent Progress of Squaraine-Based Fluorescent Materials and Their Biomedical Applications. *Symmetry* **2022**, *14*, 966. [[CrossRef](#)]
53. Wang, Y.; Geng, S.; Yan, G.; Liu, X.; Zhang, X.; Feng, Y.; Shi, J.; Qu, X. A Squaraine-Linked Zwitterionic Covalent Organic Framework Nanosheets Enhanced Poly(ethylene oxide) Composite Polymer Electrolyte for Quasi-Solid-State Li–S Batteries. *ACS Appl. Energy Mater.* **2022**, *5*, 2495–2504. [[CrossRef](#)]
54. Cheng, Z.; Lu, L.; Zhang, S.; Liu, H.; Xing, T.; Lin, Y.; Ren, H.; Li, Z.; Zhi, L.; Wu, M. Amphoteric covalent organic framework as single Li⁺ superionic conductor in all-solid-state. *Nano Res.* **2022**, *16*, 528–535. [[CrossRef](#)]
55. Du, Y.; Yang, H.; Whiteley, J.M.; Wan, S.; Jin, Y.; Lee, S.; Zhang, W. Ionic Covalent Organic Frameworks with Spiroborate Linkage. *Angew. Chem.* **2016**, *128*, 1769–1773. [[CrossRef](#)]
56. Vazquez-Molina, D.A.; Mohammad-Pour, G.S.; Lee, C.; Logan, M.W.; Duan, X.; Harper, J.K.; Uribe-Romo, F.J. Mechanically Shaped 2-Dimensional Covalent Organic Frameworks Reveal Crystallographic Alignment and Fast Li-Ion Conductivity. *J. Am. Chem. Soc.* **2016**, *138*, 9767–9770. [[CrossRef](#)] [[PubMed](#)]
57. Usiskin, R.; Lu, Y.; Popovic, J.; Law, M.; Balaya, P.; Hu, Y.-S.; Maier, J. Fundamentals, status and promise of sodium-based batteries. *Nat. Rev. Mater.* **2021**, *6*, 1020–1035. [[CrossRef](#)]
58. Min, X.; Xiao, J.; Fang, M.; Wang, W.; Zhao, Y.; Liu, Y.; Abdelkader, A.M.; Xi, K.; Kumar, R.V.; Huang, Z. Potassium-ion batteries: Outlook on present and future technologies. *Energy Environ. Sci.* **2021**, *14*, 2186–2243. [[CrossRef](#)]
59. You, C.; Wu, X.; Yuan, X.; Chen, Y.; Liu, L.; Zhu, Y.; Fu, L.; Wu, Y.; Guo, Y.-G.; van Ree, T. Advances in rechargeable Mg batteries. *J. Mater. Chem. A* **2020**, *8*, 25601–25625. [[CrossRef](#)]

60. Elia, G.A.; Kravchyk, K.V.; Kovalenko, M.V.; Chacón, J.; Holland, A.; Wills, R.G. An overview and prospective on Al and Al-ion battery technologies. *J. Power Sources* **2021**, *481*, 228870. [[CrossRef](#)]
61. Wang, N.; Wan, H.; Duan, J.; Wang, X.; Tao, L.; Zhang, J. A review of zinc-based battery from alkaline to acid. *Mater. Today Adv.* **2021**, *11*, 100149. [[CrossRef](#)]

Disclaimer/Publisher's Note: The statements, opinions and data contained in all publications are solely those of the individual author(s) and contributor(s) and not of MDPI and/or the editor(s). MDPI and/or the editor(s) disclaim responsibility for any injury to people or property resulting from any ideas, methods, instructions or products referred to in the content.